J|A|C|S
ARTICLES

Published on Web 08/14/2009

A Pillared-Layer Coordination Polymer with a Rotatable Pillar Acting as a Molecular Gate for Guest Molecules

Joobeom Seo,[†] Ryotaro Matsuda,[‡,§] Hirotoshi Sakamoto,[†] Charlotte Bonneau,[‡,§] and Susumu Kitagawa*[,†,‡,§]

Department of Synthetic Chemistry and Biological Chemistry, Graduate School of Engineering, Kyoto University, Katsura, Nishikyo-ku, Kyoto 615-8510, Japan, ERATO Kitagawa Integrated Pores Project, Science and Technology Agency (JST), Kyoto Research Park Bldg #3, Shimogyo-ku, Kyoto, 600-8815, Japan, and Institute for Integrated Cell-Material Science (iCeMS), Kyoto University, Yoshida, Sakyo-ku, Kyoto 606-8501, Japan

Received May 29, 2009; E-mail: kitagawa@sbchem.kyoto-u.ac.jp

Abstract: The design of pore properties utilizing flexible motifs and functional groups is of importance to obtain porous coordination polymers with desirable functions. We have prepared a 3D pillared-layer coordination polymer, $\{[Cd_2(pzdc)_2\mathbf{L}(H_2O)_2]\cdot 5(H_2O)\cdot(CH_3CH_2OH)\}_n$ (**1**, H_2pzdc = 2,3-pyrazinedicarboxylic acid; **L** = 2,5-bis(2-hydroxyethoxy)-1,4-bis(4-pyridyl)benzene) showing (i) a rotatable pillar bearing ethylene glycol side chains acting as a molecular gate with locking/unlocking interactions triggered by guest inclusion between the side chains, (ii) framework flexibility with slippage of the layers, and (iii) coordinatively unsaturated metal centers as guest accessible sites through the removal of the water coligands. The framework clearly shows reversible single-crystal-to-single-crystal transformations in response to the removal and rebinding of guest molecules, the observation of these processes has provided fundamental clues to the understanding of the sorption profiles. The X-ray structures indicate that the 3D host framework is retained during the transformations, involving mainly rotation of the pillars and slippage of the layers. The structure of dried form **2**, $[Cd_2(pzdc)_2\mathbf{L}]_n$, has no void volume and no water coligands. Interestingly, the adsorption isotherm of water for **2** at 298 K exhibits three distinct steps coinciding with the framework functions. Compound **2** favors the uptake of CO_2 (195 K) over N_2 (77 K) and O_2 (77 K). Above all, we report on a molecular gate with a rotational module exhibiting a locking/unlocking system which accounts for gate-opening type sorption profiles.

Introduction

Recently, porous coordination polymers (PCPs) and metal-organic frameworks (MOFs) have attracted much attention[1−9] not only because they represent a unique platform for the fundamental study of novel phenomena occurring in nanometer-sized confined space, but also for their potential applications such as storage,[10−21] separation,[22−30] catalysis,[31−40] and molecular arrays.[41−48] Among various industrial applications, the separation or purification of gases or vapors demand specific

[†] Department of Synthetic Chemistry and Biological Chemistry, Graduate School of Engineering, Kyoto University.
[‡] Japan Science and Technology Agency (JST).
[§] Institute for Integrated Cell-Material Science (iCeMS), Kyoto University.

(1) Bradshaw, D.; Claridge, J. B.; Cussen, E. J.; Prior, T. J.; Rosseinsky, M. J. *Acc. Chem. Res.* **2005**, *38*, 273–282.
(2) Yaghi, O. M.; O'Keeffe, M.; Ockwig, N. W.; Chae, H. K.; Eddaoudi, M.; Kim, J. *Nature* **2003**, *423*, 705–714.
(3) Férey, G.; Mellot-Draznieks, C.; Serre, C.; Millange, F. *Acc. Chem. Res.* **2005**, *38*, 217–225.
(4) Dalgarno, S. J.; Power, N. P.; Atwood, J. L. *Coord. Chem. Rev.* **2008**, *252*, 825–841.
(5) Suh, M. P.; Cheon, Y. E.; Lee, E. Y. *Coord. Chem. Rev.* **2008**, *252*, 1007–1026.
(6) Perry IV, J. J.; Perman, J. A.; Zaworotko, M. J. *Chem. Soc. Rev.* **2009**, *38*, 1400–1417.
(7) Rosseinsky, M. J. *Microporous Mesoporous Mater.* **2004**, *73*, 15–30.
(8) Férey, G. *Chem. Soc. Rev.* **2008**, *37*, 191–214.
(9) Kitagawa, S.; Kitaura, R.; Noro, S.-i. *Angew. Chem., Int. Ed.* **2004**, *43*, 2334–2375.
(10) Beobide, G.; Wang, W.-g.; Castillo, O.; Luque, A.; Román, P.; Tagliabue, G.; Galli, S.; Navarro, J. A. R. *Inorg. Chem.* **2008**, *47*, 5267–5277.
(11) Chandler, B. D.; Enright, G. D.; Udachin, K. A.; Pawsey, S.; Ripmeester, J. A.; Cramb, D. T.; Shimizu, G. K. H. *Nat. Mater.* **2008**, *7*, 229–235.
(12) Dalrymple, S. A.; Shimizu, G. K. H. *J. Am. Chem. Soc.* **2007**, *129*, 12114–12116.
(13) Kondo, M.; Yoshitomi, T.; Seki, K.; Matsuzaka, H.; Kitagawa, S. *Angew. Chem., Int. Ed.* **1997**, *36*, 1725–1727.
(14) Morris, R. E.; Wheatley, P. S. *Angew. Chem., Int. Ed.* **2008**, *47*, 4966–4981.
(15) Murray, L. J.; Dincă, M.; Long, J. R. *Chem. Soc. Rev.* **2009**, *38*, 1294–1314.
(16) Park, Y. K.; et al. *Angew. Chem., Int. Ed.* **2007**, *46*, 8230–8233.
(17) Rowsell, J. L. C.; Yaghi, O. M. *Angew. Chem., Int. Ed.* **2005**, *44*, 4670–4679.
(18) Sava, D. F.; Kravtsov, V. C.; Nouar, F.; Wojtas, L.; Eubank, J. F.; Eddaoudi, M. *J. Am. Chem. Soc.* **2008**, *130*, 3768–3770.
(19) Tabares, L. C.; Navarro, J. A. R.; Salas, J. M. *J. Am. Chem. Soc.* **2001**, *123*, 383–387.
(20) Taylor, J. M.; Mahmoudkhani, A. H.; Shimizu, G. K. H. *Angew. Chem., Int. Ed.* **2007**, *46*, 795–798.
(21) Banerjee, R.; Phan, A.; Wang, B.; Knobler, C.; Furukawa, H.; O'Keeffe, M.; Yaghi, O. M. *Science* **2008**, *319*, 939–943.
(22) Bae, Y.-S.; Mulfort, K. L.; Frost, H.; Ryan, P.; Punnathanam, S.; Broadbelt, L. J.; Hupp, J. T.; Snurr, R. Q. *Langmuir* **2008**, *24*, 8592–8598.

 10.1021/ja904363b CCC: $40.75

materials displaying some highly guest-selective adsorption behaviors.[49−52] This requirement can be addressed by the preparation of suitable PCPs which can specifically recognize or distinguish guest molecules. The main advantage of PCPs over other microporous compounds such as zeolites or activated carbons resides in the opportunity to control the pore surface properties. It is in principle possible, for example, to adjust the degree of flexibility (or rigidity) and hydrophobicity (or hydrophilicity) of the pores, by the functionalization of the organic ligands.[53−59] Naturally, much effort has been devoted to combining PCPs intrinsic characteristics (regularity and high surface area) with the introduction of various functional groups such as coordinatively unsaturated metal centers[60−69] (UMCs) or functional organic sites[70−79] (FOSs) onto the pore surface to attribute Lewis acidity, Lewis basicity, catalytic activity,[65,70,71] and to enhance sorption properties,[66−69,79] therefore, yielding a varied array of desirable and sophisticated porous materials.

In addition to the presence of chemical functionalities on the pore surface, flexible PCPs can undergo several types of dynamic structural changes resulting in high selectivity for guest inclusion,[50,52,80] hysteretic sorption,[81,82] stepwise guest uptake[83−86]

(23) Bárcia, P. S.; Zapata, F.; Silva, J. A. C.; Rodrigues, A. E.; Chen, B. *J. Phys. Chem. B* **2007**, 6101–6103.
(24) Bastin, L.; Barcia, P. S.; Hurtado, E. J.; Silva, J. A. C.; Rodrigues, A. E.; Chen, B. *J. Phys. Chem. C* **2008**, *112*, 1575–1581.
(25) Bradshaw, D.; Prior, T. J.; Cussen, E. J.; Claridge, J. B.; Rosseinsky, M. J. *J. Am. Chem. Soc.* **2004**, *126*, 6106–6114.
(26) Chen, B.; Liang, C.; Yang, J.; Contreras, D. S.; Clancy, Y. L.; Lobkovsky, E. B.; Yaghi, O. M.; Dai, S. *Angew. Chem., Int. Ed.* **2006**, *45*, 1390–1393.
(27) Choi, E.-Y.; Park, K.; Yang, C.-M.; Kim, H.; Son, J.-H.; Lee, S. W.; Lee, Y. H.; Min, D.; Kwon, Y.-U. *Chem.−Eur. J.* **2004**, *10*, 5535–5540.
(28) Li, J.-R.; Kuppler, R. J.; Zhou, H.-C. *Chem. Soc. Rev.* **2009**, *38*, 1477–1504.
(29) Ma, S.; Sun, D.; Wang, X.-S.; Zhou, H.-C. *Angew. Chem., Int. Ed.* **2007**, *46*, 2458–2462.
(30) Pan, L.; Olson, D. H.; Ciemnolonski, L. R.; Heddy, R.; Li, J. *Angew. Chem., Int. Ed.* **2006**, *45*, 616–619.
(31) Alaerts, L.; Séguin, E.; Poelman, H.; Thibault-Starzyk, F.; Jacobs, P. A.; Vos, D. E. D. *Chem.−Eur. J.* **2006**, *12*, 7353–7363.
(32) Cho, S.-H.; Ma, B.; Nguyen, S. T.; Hupp, J. T.; Albrecht-Schmitt, T. E. *Chem. Commun.* **2006**, 2563–2565.
(33) Fujita, M.; Kwon, Y. J.; Washizu, S.; Ogura, K. *J. Am. Chem. Soc.* **1994**, *116*, 1151–1152.
(34) Gómez-Lor, B.; Gutiérrez-Puebla, E.; Iglesias, M.; Monge, M. A.; Ruiz-Valero, C.; Snejko, N. *Chem. Mater.* **2005**, *17*, 2568–2573.
(35) Hwang, Y. K.; Hong, D.-Y.; Chang, J.-S.; Jhung, S. H.; Seo, Y.-K.; Kim, J.; Vimont, A.; Daturi, M.; Serre, C.; Férey, G. *Angew. Chem., Int. Ed.* **2008**, *47*, 4144–4148.
(36) Lee, J.; Farha, O. K.; Roberts, J.; Scheidt, K. A.; Nguyen, S. T.; Hupp, J. T. *Chem. Soc. Rev.* **2009**, *38*, 1450–1459.
(37) Ma, L.; Abney, C.; Lin, W. *Chem. Soc. Rev.* **2009**, *38*, 1248–1256.
(38) Ohmori, O.; Fujita, M. *Chem. Commun.* **2004**, 1586–1587.
(39) Wu, C.-D.; Hu, A.; Zhang, L.; Lin, W. *J. Am. Chem. Soc.* **2005**, *127*, 8940–8941.
(40) Shultz, A. M.; Farha, O. K.; Hupp, J. T.; Nguyen, S. T. *J. Am. Chem. Soc.* **2009**, *131*, 4204–4205.
(41) Kawano, M.; Kawamichi, T.; Haneda, T.; Kojima, T.; Fujita, M. *J. Am. Chem. Soc.* **2007**, *129*, 15418–15419.
(42) Kitaura, R.; Kitagawa, S.; Kubota, Y.; Kobayashi, T. C.; Kindo, K.; Mita, Y.; Matsuo, A.; Kobayashi, M.; Chang, H.-C.; Ozawa, T. C.; Suzuki, M.; Sakata, M.; Takata, M. *Science* **2002**, *298*, 2358–2361.
(43) Kitaura, R.; Matsuda, R.; Kubota, Y.; Kitagawa, S.; Takata, M.; Kobayashi, T. C.; Suzuki, M. *J. Phys. Chem. B* **2005**, *109*, 23378–23385.
(44) Kubota, Y.; Takata, M.; Matsuda, R.; Kitaura, R.; Kitagawa, S.; Kato, K.; Sakata, M.; Kobayashi, T. C. *Angew. Chem., Int. Ed.* **2005**, *44*, 920–923.
(45) Takamizawa, S.; Kachi-Terajima, C.; Kohbara, M. A.; Akatsuka, T.; Jin, T. *Chem. Asian J.* **2007**, *2*, 837–848.
(46) Takamizawa, S.; Nakata, E.; Akatsuka, T. *Angew. Chem., Int. Ed.* **2006**, *45*, 2216–2221.
(47) Takamizawa, S.; Nakata, E.; Yokoyama, H.; Mochizuki, K.; Mori, W. *Angew. Chem., Int. Ed.* **2003**, *42*, 4331–4334.
(48) Uemura, T.; Yanai, N.; Kitagawa, S. *Chem. Soc. Rev.* **2009**, *38*, 1228–1236.
(49) Chandler, B. D.; Cramb, D. T.; Shimizu, G. K. H. *J. Am. Chem. Soc.* **2006**, *128*, 10403–10412.
(50) Matsuda, R.; Kitaura, R.; Kitagawa, S.; Kubota, Y.; Belosludov, R. V.; Kobayashi, T. C.; Sakamoto, H.; Chiba, T.; Takata, M.; Kawazoe, Y.; Mita, Y. *Nature* **2005**, *436*, 238–241.
(51) Wang, B.; Côté, A. P.; Furukawa, H.; O'Keeffe, M.; Yaghi, O. M. *Nature* **2008**, *453*, 207–211.
(52) Shimomura, S.; Horike, S.; Matsuda, R.; Kitagawa, S. *J. Am. Chem. Soc.* **2007**, *129*, 10990–10991.
(53) Lin, X.; Jia, J.; Zhao, X.; Thomas, K. M.; Blake, A. J.; Walker, G. S.; Champness, N. R.; Hubberstey, P.; Schröder, M. *Angew. Chem., Int. Ed.* **2006**, *45*, 7358–7364.
(54) Kosal, M. E.; Chou, J.-H.; Wilson, S. R.; Suslick, K. S. *Nat. Mater.* **2002**, *1*, 118–121.
(55) Cairns, A. J.; Perman, J. A.; Wojtas, L.; Kravtsov, V. C.; Alkordi, M. H.; Eddaoudi, M.; Zaworotko, M. J. *J. Am. Chem. Soc.* **2008**, *130*, 1560–1561.
(56) Dincă, M.; Dailly, A.; Tsay, C.; Long, J. R. *Inorg. Chem.* **2008**, *47*, 11–13.
(57) Kitaura, R.; Onoyama, G.; Sakamoto, H.; Matsuda, R.; Noro, S.-i.; Kitagawa, S. *Angew. Chem., Int. Ed.* **2004**, *43*, 2684–2687.
(58) Noro, S.-i.; Kitagawa, S.; Yamashita, M.; Wada, T. *Chem. Commun.* **2002**, 222–223.
(59) Shimizu, G. K. H.; Vaidhyanathan, R.; Taylor, J. M. *Chem. Soc. Rev.* **2009**, *38*, 1430–1449.
(60) Chui, S. S.-Y.; Lo, S. M.-F.; Charmant, J. P. H.; Orpen, A. G.; Williams, I. D. *Science* **1999**, *283*, 1148–1150.
(61) Kitagawa, S.; Noro, S.-i.; Nakamura, T. *Chem. Commun.* **2006**, 701–707.
(62) Sakamoto, H.; Matsuda, R.; Bureekaew, S.; Tanaka, D.; Kitagawa, S. *Chem.−Eur. J.* **2009**, *15*, 4985–4989.
(63) Schlichte, K.; Kratzke, T.; Kaskel, S. *Microporous Mesoporous Mater.* **2004**, *73*, 81–84.
(64) Chen, B.; Fronczek, F. R.; Maverick, A. W. *Inorg. Chem.* **2004**, *43*, 8209–8211.
(65) Horike, S.; Dincá, M.; Tamaki, K.; Long, J. R. *J. Am. Chem. Soc.* **2008**, *130*, 5854–5855.
(66) Chen, B.; Ockwig, N. W.; Millward, A. R.; Contreras, D. S.; Yaghi, O. M. *Angew. Chem., Int. Ed.* **2005**, *44*, 4745–4749.
(67) Chen, B.; Zhao, X.; Putkham, A.; Hong, K.; Lobkovsky, E. B.; Hurtado, E. J.; Fletcher, A. J.; Thomas, K. M. *J. Am. Chem. Soc.* **2008**, *130*, 6411–6423.
(68) Lee, Y.-G.; Moon, H. R.; Cheon, Y. E.; Suh, M. P. *Angew. Chem., Int. Ed.* **2008**, *47*, 7741–7745.
(69) Wang, X.-S.; Ma, S.; Forster, P. M.; Yuan, D.; Eckert, J.; López, J. J.; Murphy, B. J.; Parise, J. B.; Zhou, H.-C. *Angew. Chem., Int. Ed.* **2008**, *47*, 7263–7266.
(70) Hasegawa, S.; Horike, S.; Matsuda, R.; Furukawa, S.; Mochizuki, K.; Kinoshita, Y.; Kitagawa, S. *J. Am. Chem. Soc.* **2007**, *129*, 2607–2614.
(71) Seo, J. S.; Whang, D.; Lee, H.; Jun, S. I.; Oh, J.; Jeon, Y. J.; Kim, K. *Nature* **2000**, *404*, 982–986.
(72) Couck, S.; Denayer, J. F. M.; Baron, G. V.; Rémy, T.; Gascon, J.; Kapteijn, F. *J. Am. Chem. Soc.* **2009**, *131*, 6326–6327.
(73) Chen, B.; Wang, L.; Xiao, Y.; Fronczek, F. R.; Xue, M.; Cui, Y.; Qian, G. *Angew. Chem., Int. Ed.* **2009**, *48*, 500–503.
(74) Custelcean, R.; Gorbunova, M. G. *J. Am. Chem. Soc.* **2005**, *127*, 16362–16363.
(75) Horike, S.; Bureekaew, S.; Kitagawa, S. *Chem. Commun.* **2008**, 471–473.
(76) Tzeng, B.-C.; Chen, B.-S.; Yeh, H.-T.; Lee, G.-H.; Peng, S.-M. *New J. Chem.* **2006**, *30*, 1087–1092.
(77) Uemura, K.; Kitagawa, S.; Fukui, K.; Saito, K. *J. Am. Chem. Soc.* **2004**, *126*, 3817–3828.
(78) Uemura, K.; Kitagawa, S.; Kondo, M.; Fukui, K.; Kitaura, R.; Chang, H.-C.; Mizutani, T. *Chem.−Eur. J.* **2002**, *8*, 3587–3600.
(79) Yang, W.; Lin, X.; Jia, J.; Blake, A. J.; Wilson, C.; Hubberstey, P.; Champness, N. R.; Schröder, M. *Chem. Commun.* **2008**, 359–361.
(80) Bourrelly, S.; Llewellyn, P. L.; Serre, C.; Millange, F.; Loiseau, T.; Férey, G. *J. Am. Chem. Soc.* **2005**, *127*, 13519–13521.
(81) Serre, C.; Bourrelly, S.; Vimont, A.; Ramsahye, N. A.; Maurin, G.; Llewellyn, P. L.; Daturi, M.; Filinchuk, Y.; Leynaud, O.; Barnes, P.; Férey, G. *Adv. Mater.* **2007**, *19*, 2246–2251.
(82) Zhao, X.; Xiao, B.; Fletcher, A. J.; Thomas, K. M.; Bradshaw, D.; Rosseinsky, M. J. *Science* **2004**, *306*, 1012–1015.
(83) Choi, H. J.; Dincá, M.; Long, J. R. *J. Am. Chem. Soc.* **2008**, *130*, 7848–7850.

and gate-opening type adsorption behaviors.[87,88] These dynamic responses either showing expansion or shrinkage of the pores are allowed by various structural motifs which fall into three main categories: (i) mechanical motifs such as interpenetration[89,90] and stacking;[91−95] (ii) chemical motifs requiring the addition, reorientation, or cleavage of a coordination bond;[96−99] and (iii) rotational modules involving bridging ligands containing parts that can undergo free rotation.[100,101] While the first two entail a complete overhaul of the frameworks and sometimes a change in dimensionality to display a change in pore geometry and volume, the latter only involves the rotation of a restricted part of the bridging ligands. In this regard, rotational modules are intrinsically different from the others as only a subtle change in the orientation of a part of the ligand can trigger drastic changes in the characteristics of the pores, not only in geometry and volume, but also in terms of accessibility; that is, rotational modules can act as local molecular-gates for guest inclusion. Reports of such materials are still scarce, whereas the others are well-documented.[102,103]

Herein, we report on the design of pore space via the introduction of a rotational module on a flexible framework. In particular, we present a 3D coordination pillared-layer structure, $\{[Cd_2(pzdc)_2\mathbf{L}(H_2O)_2]\cdot 5(H_2O)\cdot(CH_3CH_2OH)\}_n$ (**1**, H_2pzdc = 2,3-pyrazinedicarboxylic acid; **L** = 2,5-bis(2-hydroxyethoxy)-1,4-bis(4-pyridyl)benzene), showing (i) a rotatable pillar bearing ethylene glycol side chains acting as a molecular gate with locking/unlocking interactions triggered by guest inclusion (Figure 1), (ii) framework flexibility with slippage of the layers, and (iii) UMCs as guest accessible sites through the removal of the water coligand. We demonstrate how these characteristics have direct consequences on the selective, stepwise sorption, and gate-opening behaviors of the material for various guest molecules. Notably, the title compound is the first material to display a rotational module featuring a locking/unlocking mechanism of the channels depending on guest inclusion.

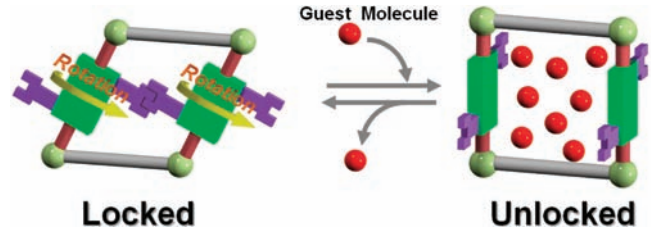

Figure 1. Design of pore space via the introduction of a rotational module as a molecular gate with locking/unlocking interactions triggered by guest inclusion.

Scheme 1. 2,5-Bis(2-hydroxyethoxy)-1,4-bis(4-pyridyl)benzene (**L**)

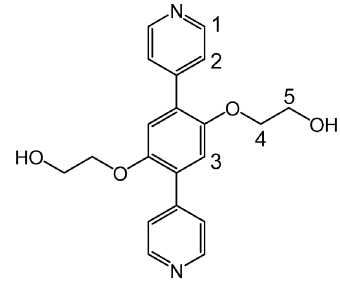

L

Results and Discussion

Synthesis and Crystal Structure. For the rational construction of porous frameworks with controlled channel dimensions, the "pillared-layer" motif has so far been employed, because simple modification of the pillars can control not only the channel size, but also chemical functionality.[42,50,87,95,97] We designed a 4-pyridine terminated rodlike ligand containing ethylene glycol side chains (**L**) as pillar (Scheme 1) that plays important roles in the resulting framework. First, the pore properties can be tuned via rotation of **L**, thereby inducing gate-opening type adsorption. Second, the guest-free framework can be stabilized by allowing ethylene glycol side chains to occupy the empty pore as guest molecules.

Compound **1** was synthesized by the reaction of $Cd(NO_3)_2$ with Na_2pzdc and **L** (1:1:1 ratio) in EtOH/H_2O 1:1 mixture as colorless crystal. Compound **1** is stable in air and insoluble in common organic solvents. It was formulated as $\{[Cd_2(pzdc)_2\mathbf{L}(H_2O)_2]\cdot 5(H_2O)\cdot(CH_3CH_2OH)\}_n$ (**1**) by single-crystal X-ray diffraction and thermogravimetric (TG) analyses. Compound **1** has two crystallographically independent Cd^{2+} ions with different coordination environments in the asymmetric unit (Figure 2a). Cd(1) is heptacoordinated, residing in a distorted pentagonal bipyramidal geometry, surrounded by four oxygen atoms, one nitrogen atom in the equatorial position from three pzdc ligands, one nitrogen atom from **L** and one water oxygen atom ligated in the axial positions. Cd(2) is hexacoordinated, residing in a distorted octahedral geometry, surrounded by three oxygen atoms, one nitrogen atom in the equatorial position from three pzdc ligands, one nitrogen atom from **L** and one water oxygen

(84) Kondo, A.; Noguchi, H.; Carlucci, L.; Proserpio, D. M.; Ciani, G.; Kajiro, H.; Ohba, T.; Kanoh, H.; Kaneko, K. *J. Am. Chem. Soc.* **2007**, *129*, 12362–12363.
(85) Uemura, K.; Yamasaki, Y.; Komagawa, Y.; Tanaka, K.; Kita, H. *Angew. Chem., Int. Ed.* **2008**, *46*, 6662–6665.
(86) Llewellyn, P. L.; Bourrelly, S.; Serre, C.; Filinchuk, Y.; Férey, G. *Angew. Chem., Int. Ed.* **2006**, *45*, 7751–7754.
(87) Kitaura, R.; Fujimoto, K.; Noro, S.-i.; Kondo, M.; Kitagawa, S. *Angew. Chem., Int. Ed.* **2002**, *41*, 133–135.
(88) Tanaka, D.; Nakagawa, K.; Higuchi, M.; Horike, S.; Kubota, Y.; Kobayashi, T. C.; Takata, M.; Kitagawa, S. *Angew. Chem., Int. Ed.* **2008**, *47*, 3914–3918.
(89) Halder, G. J.; Kepert, C. J.; Moubaraki, B.; Murray, K. S.; Cashion, J. D. *Science* **2002**, *298*, 1762–1765.
(90) Maji, T. K.; Matsuda, R.; Kitagawa, S. *Nat. Mater.* **2007**, *6*, 142–148.
(91) Biradha, K.; Hongo, Y.; Fujita, M. *Angew. Chem., Int. Ed.* **2002**, *41*, 3395–3398.
(92) Navarro, J. A. R.; Barea, E.; Rodríguez-Diéguez, A.; Salas, J. M.; Ania, C. O.; Parra, J. B.; Masciocchi, N.; Galli, S.; Sironi, A. *J. Am. Chem. Soc.* **2008**, *130*, 3978–3984.
(93) Kitaura, R.; Seki, K.; Akiyama, G.; Kitagawa, S. *Angew. Chem., Int. Ed.* **2003**, *42*, 428–431.
(94) Kondo, A.; Noguchi, H.; Ohnishi, S.; Kajiro, H.; Tohdoh, A.; Hattori, Y.; Xu, W.-C.; Tanaka, H.; Kanoh, H.; Kaneko, K. *Nano Lett.* **2006**, *6*, 2581–2584.
(95) Maji, T. K.; Uemura, K.; Chang, H.-C.; Matsuda, R.; Kitagawa, S. *Angew. Chem., Int. Ed.* **2004**, *43*, 3269–3272.
(96) Bradshaw, D.; Warren, J. E.; Rosseinsky, M. J. *Science* **2007**, *315*, 977–980.
(97) Matsuda, R.; Kitaura, R.; Kitagawa, S.; Kubota, Y.; Kobayashi, T. C.; Horike, S.; Takata, M. *J. Am. Chem. Soc.* **2004**, *126*, 14063–14070.
(98) Ghosh, S. K.; Zhang, J.-P.; Kitagawa, S. *Angew. Chem., Int. Ed.* **2007**, *46*, 7965–7968.
(99) Kaneko, W.; Ohba, M.; Kitagawa, S. *J. Am. Chem. Soc.* **2007**, *129*, 13706–13712.
(100) Horike, S.; Matsuda, R.; Tanaka, D.; Matsubara, S.; Mizuno, M.; Endo, K.; Kitagawa, S. *Angew. Chem., Int. Ed.* **2006**, *45*, 7226–7230.
(101) Lee, E. Y.; Jang, S. Y.; Suh, M. P. *J. Am. Chem. Soc.* **2005**, *127*, 6374–6381.
(102) Kitagawa, S.; Matsuda, R. *Coord. Chem. Rev.* **2007**, *251*, 2490–2509.
(103) Férey, G.; Serre, C. *Chem. Soc. Rev.* **2009**, *38*, 1380–1399.

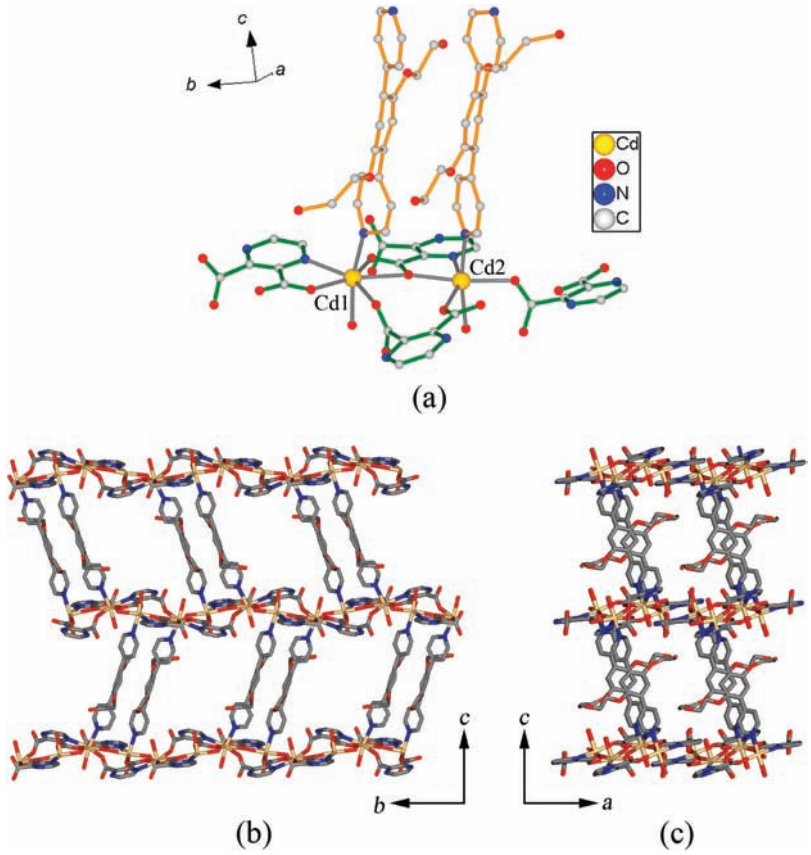

Figure 2. Structural elucidation of the as-synthesized compound **1**. (a) Atomic connectivity around the Cd^{2+} centers. (b) Top view and (c) side view of the overall 3D structure of **1**. Cd, pale yellow; O, red; N, blue; C, gray. Disordered atoms, hydrogen atoms and guest molecules are omitted for clarity.

atom ligated to axial positions. Bond distances around Cd^{2+} centers are unremarkable. Each pzdc ligand is coordinated to three Cd^{2+} centers through three oxygen and one nitrogen atoms, forming a 2D layer in the *ab* plane. The layers are pillared with the axial coordination **L**, forming a 3D network with interlayer distance of 14.89 Å (Figure 2). The paired pillars (**L**) in **1** are stabilized by aromatic interactions (distance from edge of the pyridine ring to center of the neighboring pyridine ring = 3.44−3.76 Å) as well as hydrogen bonding (C···O = 2.76−3.23 Å) among the ethylene glycol side chains. The ethylene glycol side chains are oriented on the crystallographic *ac* plane without severe disorder to form two types of channels about 10.12 × 6.01 $Å^2$ along the *a* axis and channels of 2.83 × 1.62 $Å^2$ along the *b* axis (the channel size is measured by considering van der Waals radii for constituting atoms.). The void volume calculated by PLATON[104] is 35% in which water and ethanol guest molecules are accommodated. The synthesis of **1** is heavily dependent on the concentration of each ion and can only be successful with the following molar ratio of $Cd(NO_3)_2$/Na_2pzdc/**L** = 1: 1: 1. When the concentration of **L** is halved, unidentified byproduct are formed (Figure S1).

Structure Stability. To examine the thermal stability of **1**, TG analysis and powder X-ray diffraction pattern (PXRD) measurements were carried out. The TG curve of **1** indicates the release of guest molecules up to 100 °C with a weight loss of 16.0% (calcd. 15.9%) to give the dried form **2**, $[Cd_2(pzdc)_2\mathbf{L}]_n$. At 245 °C, the framework starts to collapse,

(104) Spek, A. L. *Acta Crystallogr., Sect. A* **1990**, *46*, 194–201.

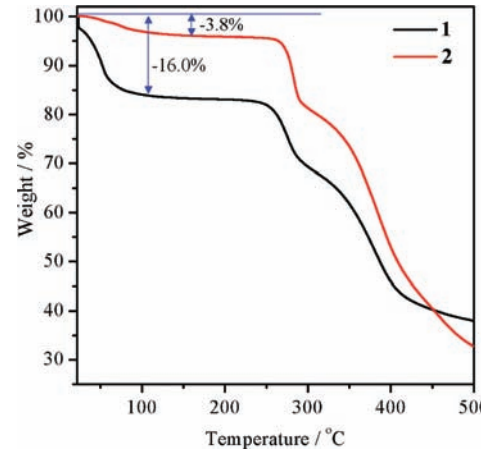

Figure 3. TGA profiles of **1** and **2** with a heating rate of 5 °C min^{-1}.

but no chemical decomposition was observed between the desolvation and degradation temperatures (Figure 3). The TG curve of **2** shows a 3.8% of weight loss, which is equivalent to two water molecules per formula unit, corresponding to the coordination of atmospheric H_2O to two Cd^{2+} centers per formula unit of **2** at room temperature (Figure 3). The TG curve of **2** recorded in air also supports this result by showing both weight loss and weight increase in response to temperature (Figure S2). Figure 4 shows the observed PXRD patterns of **1** and **2**. PXRD pattern of **1** measured at 298 K is in good agreement with that of simulated pattern obtained from the single-crystal structure. PXRD pattern of **2** measured at 383 K shows diffraction peaks indicating that the framework is

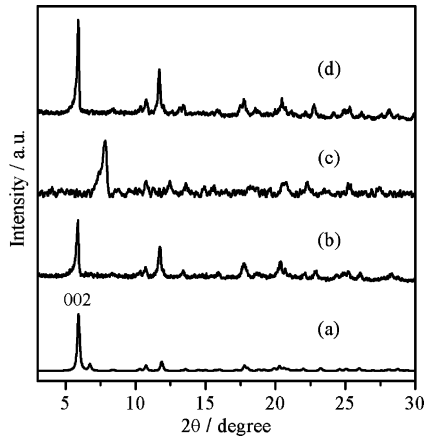

Figure 4. PXRD patterns of (a) simulated pattern from single-crystal structure of **1**, (b) as-synthesized **1**, (c) drying of **1** in *vacuo* at 383 K for 3 h (**2**), (d) **2** exposed to H_2O.

maintained even without guest molecules. However, the 002 reflection, corresponding to the interlayer distance, shifts from 6.2° for **1** to 7.4° for **2**, which indicates a decrease in the interlayer distance. To test the reversibility of the structural transformation, **2** was exposed to water vapor. Interestingly, the PXRD pattern of **2** could be regenerated by water after 1 day as shown in Figure 4d.

Single-Crystal-to-Single-Crystal Transformations of 1. The structural transformations of **1** upon desolvation and rehydration are shown in Figures 5 and 6. Single crystals of **1** remain physically intact after 1 day under N_2 atmosphere at room temperature but yield to single crystals of the partially dried form **1a**, $\{[Cd_2(pzdc)_2\mathbf{L}(H_2O)_2]\cdot 3(H_2O)\cdot(CH_3CH_2OH)\}_n$. The structure determination of **1a** shows a decrease of the cell volume (714.0 Å^3, 15.4%) and a reduction of the *c* axis (3.98 Å, 13.3%). The connectivity of the framework is same as that of **1**. Nevertheless, compound **1a** exhibits an interesting slippage of the layers (interlayer distance = 12.68 Å) with a tilting and rotation of the pillar from the crystallographic *ac* plane for **1** to the *bc* plane for **1a**. The void volume occupied by ethanol and water molecules is 8.2% (Table 1).

Compound **1** retains single crystallinity even when the single crystal of **1** is desolvated at high temperature (110 °C) under Ar atmosphere and gives the dried form **2**, $[Cd(pzdc)_2\mathbf{L}]_n$. These crystals were analyzed under continuous heating at 110 °C. The structure determination of **2** shows that the space group is preserved, but the cell volume (1290.4 Å^3, 27.9%) and *c* axis (7.65 Å, 25.6%) are significantly smaller compared to **1**. The connectivity of pzdc and pillar **L** are also preserved. On the other hand, the coordination environment of the two Cd^{2+} centers is changed due to the loss of the coordinated water molecules. Cd(1) has a distorted octahedral geometry, and Cd(2) has a distorted square pyramidal environment (Figure 6). The 2D layer of **2**, $[Cd(pzdc)]_n$, also shows a structural transformation to form a corrugated layer. The rotated pillars are stabilized by hydrogen bonding between the hydroxyl groups with a distance of 2.947(18) Å even at 110 °C (Figure S3). Note that compound **2** is not porous, as can be seen from the crystal structure; the void volume is 2%.

Compound **2** is transformed to the expanded-intermediate form **3**, $\{[Cd_2(pzdc)_2\mathbf{L}(H_2O)_2]\cdot 5(H_2O)\}_n$, after exposure to water vapor at room temperature for about 6 h. The crystal structure of **3** shows that the cell volume undergoes a 17.8% (593.9 Å^3) increase and likewise the *c* axis increases by 16.8% (3.73 Å),

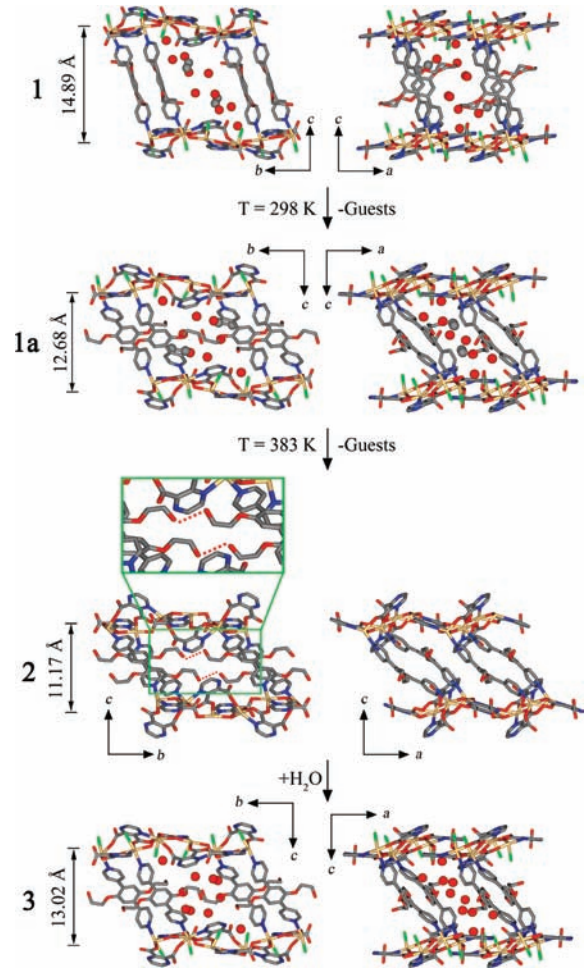

Figure 5. Crystal structure of **1**, **1a**, **2**, and **3** showing structural transformations upon desolvation and rehydration. The red dashed lines in the crystal structure of **2** mean the hydrogen bonds. Cd, pale yellow; O, red; N, blue; C, gray; coordinated water, green. Hydrogen atoms are omitted for clarity.

but the original symmetry is retained. The connectivity of the ligands is the same as found in **1** and **1a**. The coordination geometry of the two Cd^{2+} centers changes due to the coordination of water molecules. Cd(1) has a distorted pentagonal bipyramidal geometry, and Cd(2) has a distorted octahedral environment (Figure 6). Compound **3** shows a slippage of the layers (interlayer distance = 13.02 Å) responsible for the expansion of the framework compared to **2**. The 2D layer of **3**, $[Cd_2(pzdc)_2(H_2O)_2]_n$, is less corrugated than that of **2**. The void volume is occupied by water molecules (10%) which are stabilized by hydrogen bonds with the carboxylate and hydroxyl oxygen atoms (O···O = 2.77−3.08 Å) (Figure S4).

Sorption Properties. The adsorption isotherms of the dried form **2** were measured for the sorption of water and methanol at 298 K to assess the impact of the structural transformations of the framework. The water sorption isotherm of **2** shown in Figure 7 is characterized by three unequivocal steps and a large hysteresis. To follow the structural transformations of **2** upon adsorption of water, *in situ* PXRD experiments under various vapor pressures of water were carried out (Figure 7). The two water molecules adsorbed during the first step in the lower pressure region, $P/P_0 = 0-0.16$, correspond to the coordination of two water molecules to two Cd^{2+} centers per formula unit; these are the UMCs as guest-accessible sites. The PXRD pattern

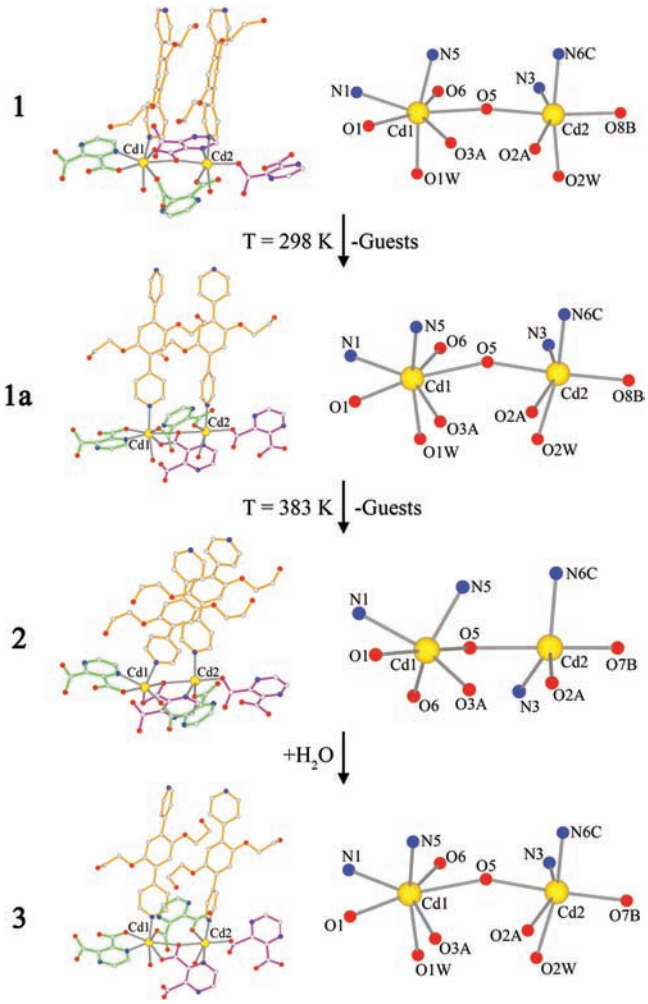

Figure 6. View of the ligand coordination modes (left) and the coordination geometries of the two crystallographically independent Cd^{2+} centers (right) of **1**, **1a**, **2**, and **3**. Cd, pale yellow; O, red; N, blue; C, gray. Noncoordinated solvent molecules, disordered atoms, and hydrogen atoms are omitted for clarity.

at 0.63 kPa, $P/P_0 = 0.20$ at point II (Figure 7b) is unchanged, indicating that the structure of **2** is preserved despite the coordination of the two water molecules. The second uptake between $P/P_0 = 0.25-0.82$ is associated with the expanded-intermediate form (**3**), which possesses an increased pore volume due to the expansion of the interlayer distance upon adsorption. The amount adsorbed corresponds to five water molecules per formula unit. The 002 reflection in the PXRD pattern corresponding to the interlayer distance shifts from 7.4° for **2** to 6.7° (Figure 7c), thus, indicating an increase in the interlayer distance. The simulated pattern obtained from the crystal structure of **3** reproduces the peaks observed in the experimental PXRD pattern (Figure 8). However, the mismatch of some peak positions can be explained by the presence of a mixture of the compound at different stages of rehydration. The TG curve of **3** indicates desorption of six water molecules (observed 10.4%, calcd. 10.6%) at temperatures below 110 °C, which corresponds to second plateau at around 5−7 molecules per formula unit in water adsorption isotherm (Figure S5). Because of instrumental limitations, we could not collect PXRD patterns in the higher vapor pressure region (>2.50 kPa). Instead, compound **3** was exposed to water at room temperature for an additional day to give the fully rehydrated form; thereupon, the crystals lost transparency and were not suitable for single crystal X-ray analysis. The resulting PXRD pattern closely approximates that of **1**. Therefore, we presume that the third adsorption step can be attributed to the rotation of ethylene glycol side chains together with a further expansion of the framework, the same as that of **1**.

Considering both results from X-ray analyses and adsorption isotherms obtained for water, the mechanism of water adsorption operating in **2** can be explained as follows (Figure 9): in the pressure range $P/P_0 = 0-0.16$, two water molecules coordinate to two Cd^{2+} centers per formula unit, with the preservation of the framework and most probably of the hydrogen bonding interactions between the ethylene glycol side chains, that is; the channels are still locked, nevertheless, some water adsorption can still occur as water molecules are small. A further increase of the adsorption pressure after $P/P_0 = 0.20$ causes the expansion of the framework upon adsorption of water molecules in the channels to form the expanded-intermediate form **3**. The crystal structure of **3** (Figure 5) shows that, while the orientation of ethylene glycol side chains at this stage remains unchanged, the hydrogen bond between the ethylene glycol side chains is

Table 1. Crystal Data and Structure Refinement for **1**, **1a**, **2**, and **3**

	1	1a	2	3
Formula	$C_{34}H_{42}Cd_2N_6O_{19}$	$C_{34}H_{34}Cd_2N_5O_{18}$	$C_{32}H_{24}Cd_2N_6O_{12}$	$C_{32}H_{34}Cd_2N_6O_{17}$
M_r	1063.54	1025.46	909.37	999.45
Crystal system	Monoclinic	Monoclinic	Monoclinic	Monoclinic
Space group	$P2_1/c$	$P2_1/n$	$P2_1/n$	$P2_1/n$
a [Å]	10.6150(11)	10.236(2)	10.701(8)	10.261(2)
b [Å]	14.5889(15)	14.827(3)	14.170(11)	14.825(3)
c [Å]	29.856(3)	25.877(5)	22.205(17)	25.931(5)
β [deg]	90.395(17)	95.45(3)	98.117(13)	95.40(3)
V [Å^3]	4623.4(8)	3909.4(14)	3333.0(40)	3926.9(14)
Z	4	4	4	4
ρ_{calcd} [g cm^{-3}]	1.528	1.742	1.812	1.691
$F(000)$	2144	2052	1800	2000
μ [mm^{-1}]	0.996	1.172	1.350	1.163
T [K]	93.15	93.15	378.15	93.15
2θ range	6.14−55.00°	6.00−54.98°	6.04−54.92°	6.32−55.08°
GOF	1.056	1.074	1.099	1.073
Reflections collected	33416	31569	23226	30058
Independent reflections	10367	8851	7185	8957
*R*int	0.0331	0.0380	0.0491	0.0727
Final $R1$, $wR2$ [$I > 2\sigma(I)$]	0.0735, 0.1874	0.0663, 0.1766	0.1006, 0.2613	0.1202, 0.2961
(all data)	0.0735, 0.0735	0.0849, 0.1954	0.1280, 0.2911	0.1597, 0.3400
Parameters	630	538	469	532

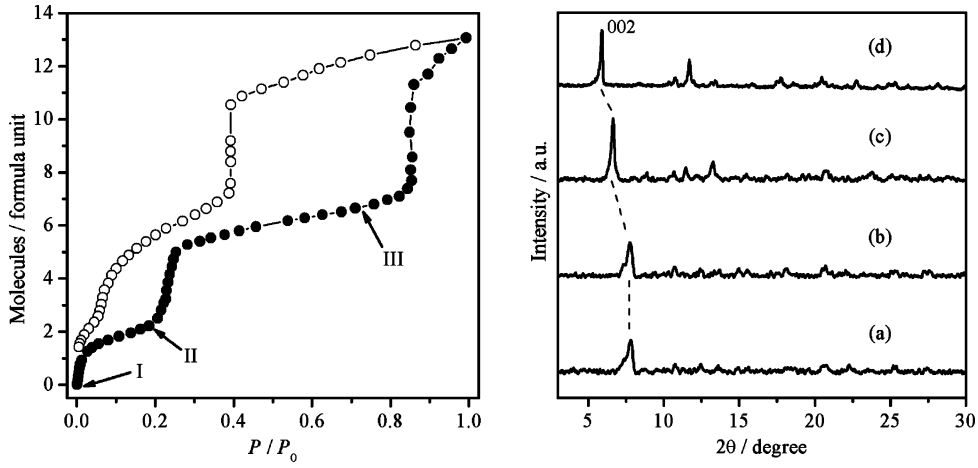

Figure 7. Isotherm (left) of the vapor adsorption (●) and desorption (○) of water on **2** (at 298 K), and PXRD patterns (right, 298 K) of **2** (a) at point I (0.00 kPa, $P/P_0 = 0.00$, dried form **2**), (b) at point II (0.54 kPa, $P/P_0 = 0.20$), (c) at point III (2.50 kPa, $P/P_0 = 0.72$, expanded-intermediate form **3**), (d) fully rehydrated form. The sample of the fully rehydrated form was obtained by exposure of **3** to water vapor at room temperature for 1 day.

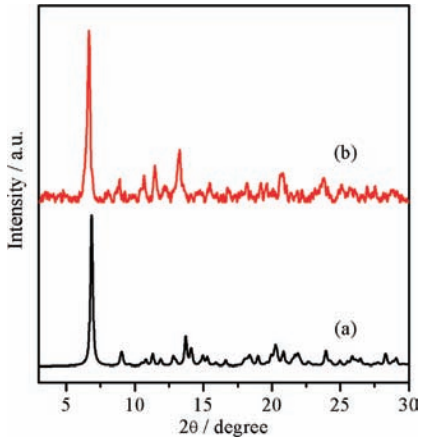

Figure 8. PXRD patterns of (a) the simulated pattern from single-crystal structure of expanded-intermediate form **3**, (b) the dried form **2** under 2.50 kPa ($P/P_0 = 0.72$, point III in Figure 7) of water vapor at 298 K.

cleaved (O···O = 4.946 Å): the gate is now unlocked, and the pillars are free to rotate. After $P/P_0 = 0.84$, the threshold for gate-opening is reached: the ethylene glycol side chains have probably significantly rotated, a further expansion of the framework is observed, and as a consequence, the framework starts to adsorb more. The PXRD of the fully rehydrated form is now identical to that of the as-synthesized compound **1**.

The desorption isotherm does not retrace the adsorption profile; only two steps occur at $P/P_0 = 0.393$ and 0.358 (Figure 7). This is unsurprising as the coordinated water molecules are not expected to leave the framework at 298 K. Structural transformations equivalent to those observed from as-synthesized **1** to the partially dried form **1a** may account for the first abrupt decrease.

The adsorption isotherm of methanol for **2** at 298 K shows a distinct two-step adsorption (Figure 10). The first step in the lower pressure region is equivalent to approximately 1.8 molecules per formula unit and corresponds to the binding of MeOH molecules to two Cd^{2+} centers in **2**. Then, the adsorption proceeds directly to approximately the same saturation level that is observed in the water sorption case (Figure 11). The absence of a second intermediate step in the methanol case may be explained by the difference in molecular volume of the two sorbates. The molecular volume of a methanol molecule (~40 Å^3) is twice the volume of a water molecule. Therefore, it is reasonable to assume that the adsorption proceeds with concurrent rotation of the pillars and framework expansion at once. The PXRD pattern of the dried form **2** measured after MeOH soaking at 298 K shows a shift of the 002 reflection from 7.4 to 6.5° (Figure 12), which indicates an increase in the interlayer distance.

The adsorption isotherms of **2** were also measured for sorption of N_2 (at 77 K), O_2 (at 77 K), and CO_2 (at 195 K). The adsorption isotherms for O_2 (kinetic diameter = 3.46 Å)[105] and N_2 (3.64 Å) at 77 K show no uptake (Figure 13), indicating that there is no porosity in **2** corroborating the structure determination. In contrast, CO_2 (3.3 Å) regardless of its comparable size with O_2 and N_2 can be adsorbed (Figure 13). Moreover, the isotherm shows a sudden increase at $P/P_0 = 0.9$ and exhibits a large hysteresis. To gain insight into the structural transformation of **2** upon CO_2 adsorption, PXRD experiments under various pressures of CO_2 were conducted (Figure 14). The PXRD diffraction pattern at 77 kPa ($P/P_0 = 0.74$) shows the apparition of new peaks, indicating that CO_2 is adsorbed into the framework with a structural transformation. The results from repeated CO_2 adsorption measurements on the same sample show reproducibility with a small difference in onset pressure and amount (Figure 14). This abrupt inclusion of CO_2 at higher vapor pressure region can probably be explained as follows; the molecular gate in compound **2** is strongly locked by the hydrogen bond, which cannot be broken by CO_2 at low vapor pressure due to its limited ability to form hydrogen bonds compared to both water and methanol which interfere with the hydrogen bonding interactions in compound **2** as previously demonstrated. Therefore, the gate only opens at a higher vapor pressure of CO_2 ($P/P_0 = 0.9$). The adsorption isotherm of CO_2 on **2** was also measured at higher temperature (293 K). At 293 K, the gate in compound **2** opens at a lower relative vapor pressure ($P/P_0 = 0.07$, 0.4 MPa) as shown by the sudden increase in the adsorption isotherm. Most probably the increased thermal energy of both the framework and guest molecule allows CO_2 to open the hydrogen bonded gate more easily (Figure S6).

Conclusions

We have synthesized a 3D pillared-layer coordination polymer with a specifically designed pillar ligand (**L**) in order to show three specific properties. First, the ligand in response to guest

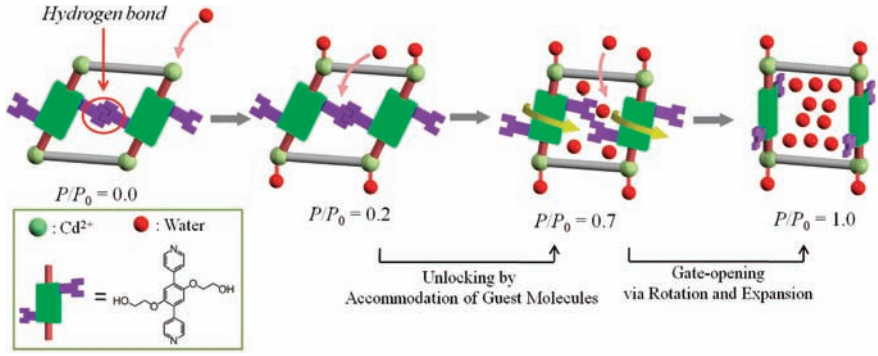

Figure 9. Schematic representation of the structural transformations triggered by water adsorption. The dashed red line between two OH means hydrogen bonding interaction.

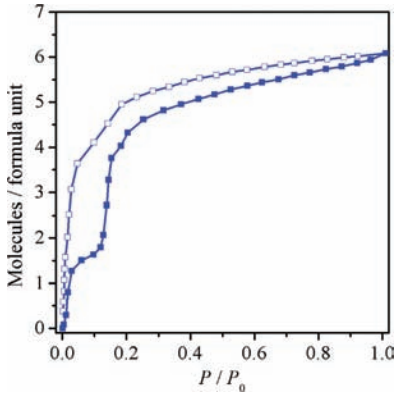

Figure 10. Adsorption (■) and desorption (□) isotherms of methanol at 298 K for **2**.

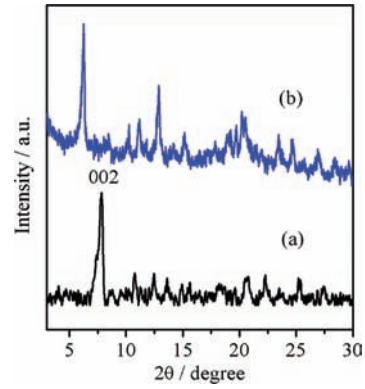

Figure 12. PXRD patterns of (a) the dried form **2** and (b) **2** after soaking in MeOH at 298 K.

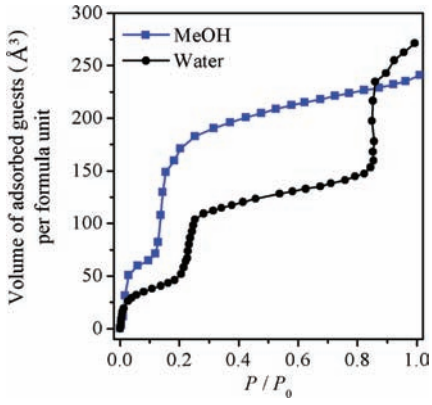

Figure 11. Comparison of volume (Å^3) of adsorbed guests in **2**. The molecular volume of one molecule of MeOH and one molecule of water was estimated from Connolly surface areas, corresponding to 39.6 and 20.8 Å^3, respectively. Connolly surface areas were calculated with Materials Studio (version 4.0, Accelrys, San Diego, CA).

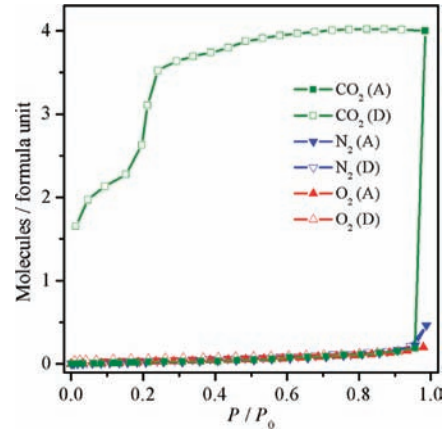

Figure 13. Adsorption (A) and desorption (D) isotherms of CO_2 (195 K), N_2 (77 K), and O_2 (77 K) for **2**.

inclusion plays the role of a molecular gate with locking/unlocking interactions. Second, the framework flexibility allows for the slippage of the layers, and finally, the removal of the water coligands provides an unsaturated metal site accessible by guest molecules. The framework clearly shows reversible single-crystal-to-single-crystal transformations in response to removal and rebinding of guest molecules, involving mainly rotation of pillars and slippage of the layers. The observation of these processes has provided fundamental clues to the understanding of the sorption profiles. We have highlighted gate-opening type sorption behaviors for water and methanol on the dried form **2**, thereby demonstrating the role of framework functions, especially the rotation of the pillar acting as molecular gate with a lock. Compound **2** can selectively adsorb carbon dioxide with large hysteresis by means of structural transformation and reject nitrogen, and oxygen. The making of a molecular gate with a rotational module exhibiting a locking/unlocking system can be regarded as an approach for the generation of previously undeveloped advanced porous materials.

Experimental Section

General Methods. All chemicals and solvents used in the syntheses were of reagent grade and were used without further purification. The ^{1}H and ^{13}C NMR spectra were recorded with a JEOL JNM-ECS400 (400 MHz) NMR spectrometer. HRMS was obtained on a JEOL JMS-700 spectrometer. The elemental analysis

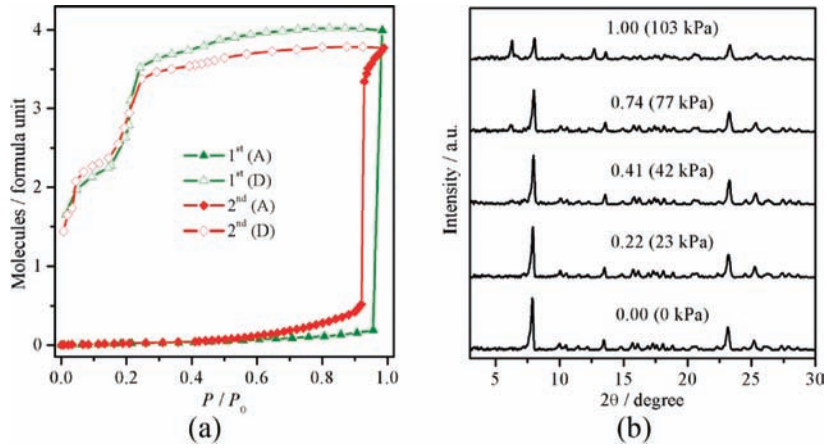

Figure 14. (a) Repeated adsorption (A) and desorption (D) isotherms of CO_2 (195 K) for **2**. (b) *In situ* PXRD patterns of **2** with adsorption of CO_2 at 195 K. The values refer to the relative pressure (P/P_0) of CO_2 at 195 K.

was carried out on a Flash EA 1112 series, Thermo Finnigan instrument. The powder X-ray diffractions (PXRD) were recorded with a Rigaku RINT-2000 Ultima diffractometer equipped with graphite monochromated Cu Kα radiation (λ = 1.54073 Å). Thermogravimetic analyses were recorded on a Rigaku Thermo plus TG-8120 apparatus in the temperature range between 298 and 773 K at a heating rate of 5 K min^{-1}. The void volumes of crystal structures were estimated by PLATON.[104]

Synthesis and Characterization of 2,5-Bis(2-hydroxyethoxy)-1,4-bis(4-pyridyl)benzene (L). 1,4-Diiodo-2,5-dihydroxybenzene was prepared according to literature method.[106] A mixture of 1,4-diiodo-2,5-dihydroxybenzene (0.70 g, 1.56 mmol), 4-pyridylboronic acid ester (0.85 g, 4.15 mmol), K_3PO_4 (2.57 g, 12.1 mmol) and $Pd(PPh_3)_4$ (300 mg) in 1,4-dioxane (100 mL) was refluxed under N_2 atmosphere for 2 days. After removal of the solvent, the residue was purified by flash column chromatography on a silica gel using methanol/dichloromethane (1:9) as eluent to give a pale yellow solid in 60% yield (0.33 g, 0.94 mmol). ^{1}H NMR (DMSO-d_6): δ 8.62 (*d*, 4H, H_1), 7.71 (*d*, 4H, H_2), 7.22 (*s*, 2H, H_3), 4.85 (*t*, 2H, O*H*), 4.10 (*t*, 4H, H_4), 3.68 (*m*, 4H, H_5). ^{13}C NMR (DMSO-d_6): δ 149.9, 149.3, 144,8, 128.0, 124.0, 115.6, 70.8, 59.4. HRMS (FAB) *m*/*z* calcd. for $C_{20}H_{21}N_2O_4$ ($M + H^+$), 323.1501; found, 353.1497. The proton numbers in NMR data indicate that nonequivalent protons represented in Scheme 1.

Preparation of $\{[Cd_2(pzdc)_2L(H_2O)_2]\cdot 5(H_2O)\cdot(EtOH)\}_n$ (1) and $[Cd_2(pzdc)_2L]_n$ (2). A solution of $Cd(NO_3)_2\cdot 4H_2O$ (30.8 mg, 0.1 mmol) in EtOH/H_2O (1:1, 25 mL) was slowly and carefully added to a solution of **L** (35.2 mg, 0.1 mmol) and Na_2pzdc (21.2 mg, 0.1 mmol) in EtOH/H_2O (1:1, 25 mL). Colorless needle-shaped crystals of **1** were obtained after 1 week. Crystals were separated and washed with EtOH/H_2O (1:1) mixture and dried. The crystals of **1** were heated to 110 °C in *vacuo* for 3 h to produce **2**. Elemental analysis (%) calcd. for **2**, $C_{32}H_{24}Cd_2N_6O_{12}$ (909.39): C, 42.26; H, 2.66%. Found, C, 42.45; H, 2.95%.

Gas Adsorption Measurements. The sorption isotherm measurements were performed using an automatic volumetric adsorption apparatus (BELSORP-max; Bel Japan, Inc.). The as-synthesized sample were evacuated under high vacuum ($<10^{-2}$ Pa) at 383 K for overnight to remove the guest molecules. The adsorbate was placed into the sample tube, then, prior to measurement, evacuated again using degas function of the analyzer for 3 h at 383 K. The change of the pressure was monitored and the degree of adsorption was determined by the decrease of the pressure at the equilibrium state.

X-ray Studies. Data were collected on Rigaku/MSC Saturn CCD diffractometer with confocal monochromated Mo Kα radiation (λ = 0.7107 Å) and processed using the CrystalClear program (Rigaku). All the structures were solved by direct methods and refined by full matrix least-squares refinement cycles on F^2 for all data using the SHELX-97.[107] Most of the disordered ethylene glycol side chain atoms in **1** and **1a** were refined isotropically and restrained using DFIX instructions. The disordered aromatic rings in **1** were restrained using SADI instructions. The crystallizing solvents in **1** were disordered and could not be satisfactorily localized. Therefore, after all of the framework atoms, which were readily obtained from difference Fourier maps, were refined, the SQUEEZE function was used to determine the contribution of the disordered solvent molecules that could not be refined to the structure factors.[104] The contribution of these species was removed from the final structure factor calculations. The single crystal of **2** was mounted on a glass fiber with a thin coat of resin, heated to 383 K, and kept at the temperature during collection of diffraction data. The framework atoms showing relatively large thermal displacement parameters in all of the crystal structures were not sensibly resolved as partial occupancy. The guest molecules in **1**, **1a**, and **3** were restrained using ISOR 0.01 instructions. Hydrogen atoms were placed in calculated positions.

Acknowledgment. Dr. J. Seo is grateful to JSPS for a postdoctoral fellowship.

Supporting Information Available: Complete ref 16. X-ray crystallographic data for **1**, **1a**, **2**, and **3**, the water guest molecule array in **3**, TG curves of **2** and **3**, ^{1}H and ^{13}C NMR spectra of **L**. This material is available free of charge via the Internet at http://pubs.acs.org.

JA904363B

(105) Beck, D. W. *Zeolite Molecular Sieves*; Wiley & Sons: New York, 1974.
(106) Wariishi, K.; Morishima, S.-i.; Inagaki, Y. *Org. Process Res. Dev.* **2003**, *7*, 98–100.
(107) Sheldrick, G. M. *SHELX-97: Program for Crystal Structure Determination*; University of Gottingen: Germany, 1997.